Rare Metal Materials and Engineering
Volume 51, Issue 9, September 2022
Available online at www.rmme.ac.cn

Science Press

Cite this article as: Li Dongsheng, Zhao Enxu, Wang Wei, et al. Recrystallization Behavior of IN690 Alloy During Hot Compression[J]. Rare Metal Materials and Engineering, 2022, 51(09): 3146-3152.

ARTICLE

Recrystallization Behavior of IN690 Alloy During Hot Compression

Li Dongsheng, Zhao Enxu, Wang Wei, Gao Pei, Liu Fan

School of Materials Science and Engineering, Jiangsu University, Zhenjiang 212013, China

Abstract: A novel high-temperature IN690 alloy was prepared by hot extrusion process, and the effects of different temperatures, strain rates, and deformations on the dynamic recrystallization (DRX) of the IN690 alloy were investigated. The isometric compression tests were conducted on the Gleeble-3500 thermal simulation test machine. The metallographic structure, grain orientation, grain boundary distribution, and the difference in the grain orientation of the IN690 alloy before and after thermal deformation were analyzed by metallographic microscope and electron backscatter diffraction. Results show that with decreasing the temperature or increasing the strain rate, the flow stress of IN690 alloy is increased. The main softening mechanism during the deformation of IN690 alloy is dynamic recovery and DRX. The proportion of the high-angle grain boundary is increased with increasing the strain or decreasing the strain rate, because obvious DRX nucleation occurs at the large true strain or relatively low strain rate.

Key words: IN690; hot compression; microstructure; flow stress; recrystallization

The IN690 alloy exhibits excellent mechanical properties, good formability, and fine cracking resistance, resulting in its widespread use in heat-transfer tubes of steam generators in nuclear power plants. Recently, a novel U-shaped IN690 alloy tube, containing higher content of Ni and lower content of Mn, Si, Al, and Ti (compared with the composition of traditional IN690 alloy), has been developed, and its stress corrosion resistance, yield strength, and tensile strength are significantly improved. This novel IN690 alloy tube ameliorates the application of ultra-long tube in on-line internal and external degreasing techniques by reducing the tube surface contaminant and decreasing the effect of tube alloy on organization. Most thermal components are prepared under the temperature-induced deformation, whose key influence factors are the deformation temperature, deformation degree, and strain rate[1]. Meanwhile, some structures change during the thermal deformation, such as dynamic recovery (DRV) and dynamic recrystallization (DRX), which ultimately affects the material properties. Hot extrusion is a key step in the manufacturing process of IN690 alloy tube, which may cause cracks due to work hardening (WH). Therefore, the study of hot working characteristics of IN690 alloy is of great significance to optimize the hot working parameters and regulate the hot deformation microstructure and properties.

Recently, the thermal deformation behavior and microstructure evolution of Ni-based superalloys have been widely studied[2]. Wang et al[3] studied the twinning and texture of IN690 alloy pipe. Gao et al[4] studied the hot working properties of nickel-based superalloys. The metallographic microscope (OM), scanning electron microscope (SEM), and electron backscatter diffraction (EBSD) are the main observation and analysis techniques to investigate the microstructure changes during metal thermal deformation[5]. Although the rheological behavior and microstructure evolution of some nickel-based superalloys have been studied, the influence of DRX and thermal deformation parameters on DRX are rarely investigated. This research analyzed the influence of thermal deformation parameters on DRX grain evolution to provide theoretical guidance for the production of IN690 alloy.

Received date: September 07, 2021
Foundation item: Jiangsu Provincial Key Laboratory of Advanced Structural Materials (hsm1304, hsm1808)
Corresponding author: Li Dongsheng, Ph. D., Assistant Researcher, School of Materials Science and Engineering, Jiangsu University, Zhenjiang 212013, P. R. China, E-mail: dsli@ujs.edu.cn

1 Experiment

The chemical composition of IN690 alloy is shown in Table 1. The specimen was cylindrical with the diameter of 8 mm and length of 12 mm (Fig. 1). The Gleeble-3500 thermal simulation test machine was used to conduct the thermal compression tests at 950~1100 °C and strain rate of 0.01~1 s^{-1}. Before loading, the specimen was firstly heated to 1100 °C at heating rate of 10 °C/s^{-1}, held for 3 min, cooled to the deformation temperature at decreasing rate of 10 °C/s^{-1}, and held for 30 s[6,7]. Hot compression tests were performed with different parameters. The true strain was 0.8 (engineering strain was 55%). The specimen was cut along the axial direction, mechanically polished, and finally chemically corroded. The corrosive liquid consisted of 30 mL HCl, 120 mL H_2O, and 10 g $FeCl_3$. The corrosion duration was 20~30 s. Next, the specimen was cleaned by alcohol and the metallographic structure could be observed. The specimen surface was mechanically polished and electrolytically corroded with 20vol% H_2SO_4 and 80vol% CH_3OH at 15~20 V for 30~40 s for EBSD analysis by Channel 5 software.

After solution treatment at 1150 °C, the IN690 alloy structure is composed of the γ austenite, as shown in Fig.2.

Table 1 Chemical composition of IN690 alloy (wt%)

C	Cr	Fe	Al	Si	Ti	Ni
0.021	29.28	9.71	0.10	0.08	0.17	Bal.

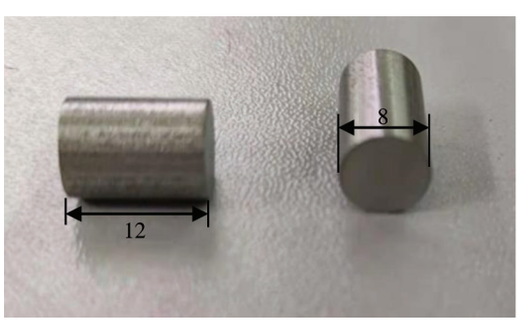

Fig.1 Schematic diagram of thermal compression specimen

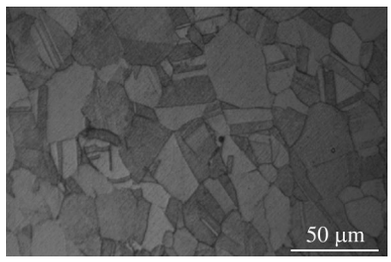

Fig.2 Solid solution grain structure of IN690 alloy

2 Results and Discussion

2.1 High-temperature compression deformation

With increasing the true strain, the true stress is firstly increased, then decreased, and finally stabilized. Additionally, the true stress is decreased with increasing the temperature, as shown in Fig. 3a. The true stress is decreased with decreasing the strain rate (Fig. 3b). When the strain rate is less than 0.1 s^{-1}, the stress reaches the maximum value and then decreased rapidly, indicating the DRX mechanism. When the strain rate is high (1 s^{-1}), the stress is slightly decreased after reaching the maximum value and tends to stabilize, indicating that DRV dominates the softening mechanism.

Both the high temperature and low strain rate can promote the grain boundary migration and enhance the driving force for nucleation and DRX grain growth[8,9]. During the thermal compression, WH phenomenon firstly occurs, and then the dynamic softening phenomena (DRV and DRX) appear[10], which is attributed to the slip and rearrangement of dislocations, thereby accelerating the stress reduction.

2.2 Thermal deformation effect on DRX grain evolution

2.2.1 Strain rate

Fig.4 shows the grain orientation imaging maps (OIMs) and misorientation analysis diagrams under different strain rates. The true strain of the deformed specimen is 0.8, and the deformation temperature is 1000 °C[11,12]. The grain evolution is sensitive to the strain rate. As shown in Fig.4a, at the strain rate of 1 s^{-1}, the deformed structure of the initial grain consists

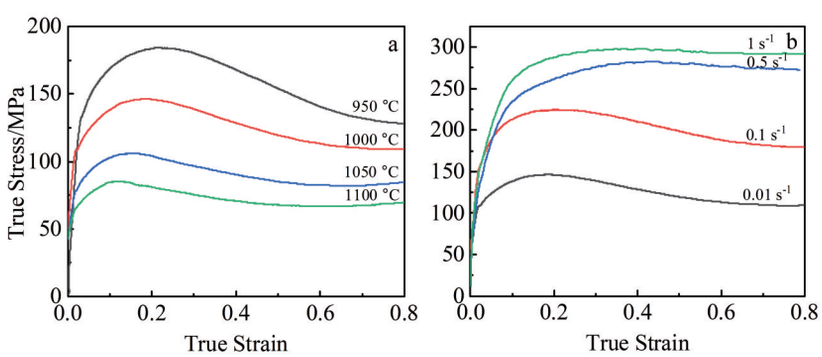

Fig.3 True stress-true strain curves of IN690 alloys under different deformation conditions: (a) strain rate=0.01 s^{-1} and (b) deformation temperature=1000 °C

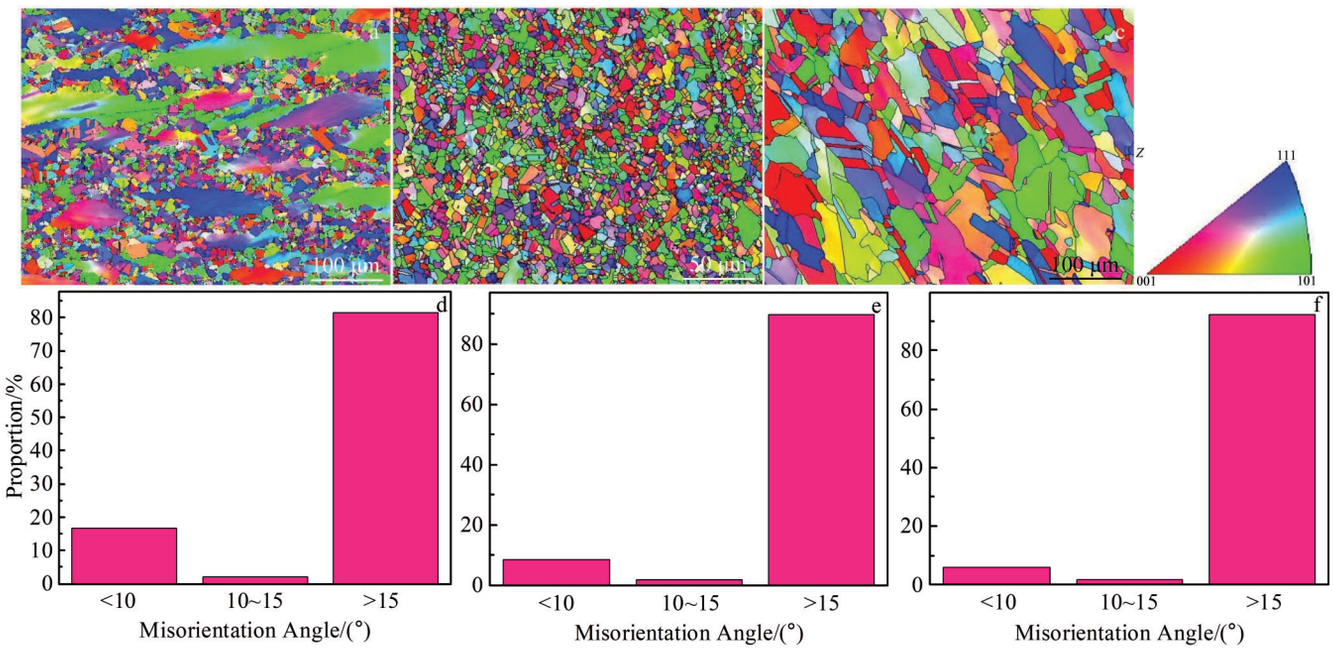

Fig.4 Grain OIMs (a~c) and misorientation analysis results (d~f) at temperature of 1000 °C and true strain of 0.8 with different strain rates: (a, d) 1 s^{-1}, (b, e) 0.1 s^{-1}, and (c, f) 0.001 s^{-1}

of some elongated original grains and some fine DRX grains[13]. However, the DRX grain size is small[14], because the high strain rate decreases the grain boundary and reduces the dislocation movement duration. Thus, DRX grain nucleation and growth are delayed.

At the strain rate of 1, 0.1, and 0.001 s^{-1}, the proportions of low-angle grain boundaries (LAGBs) are 16.6%, 8.46% and 5.87%, while the average misorientation angles are 41.01°, 42.62°, and 45.76°, respectively. With increasing the strain rate, the proportion of LAGBs is gradually increased because DRX core growth is inhibited at high strain rates[15]. The misorientation angle is increased with decreasing the strain rate, because the high strain rate induces the WH and increases the number of substructures. In addition, DRV typically possesses the relatively short latency.

2.2.2 Deformation temperature

Fig. 5 shows the grain OIMs and misorientation analysis results at different deformation temperatures under the conditions of strain rate of 0.1 s^{-1} and true strain of 0.8. The deformation temperature considerably influences the grain structure. With increasing the deformation temperature, the degree of DRX is increased. Generally, DRX nucleation is attributed to the generation, accumulation, and interaction of dislocations. Additionally, the growth of DRX grains is related to the grain movement. With increasing the deformation temperature, the dislocation evolution and grain boundary movement are increased. Therefore, at high temperatures, the degree of DRX is relatively high. At the deformation temperature of 1100 °C, most DRX grains grow (Fig.5b), and the misorientation of LAGBs is less than 15°, whereas that of the medium-angle grain boundaries (MAGBs) is 10°~15°. The high-angle grain boundaries (HAGBs) show misorientation of >15°. Thus, the deformation temperature has a considerable influence on the grain misorientation angle distribution. The average misorientation angle is 43.10° and 48.10° at 1050 and 1100 ° C, respectively. DRX nucleation is related to substructure evolution, such as dislocation annihilation. Furthermore, the structure change suggests the thermal activation process. With increasing the deformation temperature, the structure change becomes intense. Therefore, the number of DRX grains and the average misorientation angle are increased. The DRX grain growth is essential and can affect the misorientation angle, and it is controlled by the grain boundary movements.

According to Fig.5a, the initial grains almost disappear and are replaced by the refined DRX grains. The LAGBs are related to the dislocations and substructures owing to DRV mechanism. With DRX proceeding, LAGBs are gradually transformed into HAGBs. Therefore, both DRV and DRX occur during the thermal deformation. As shown in Fig.5c, the proportion of LAGBs is approximately 11.3%, indicating that the annihilation and rearrangement of dislocations are hindered at low deformation temperatures[16]. Furthermore, with increasing the deformation temperature, the crystal grains are refined. Therefore, the high deformation temperature can provide a sufficient driving force for grain boundary migration, consequently accelerating the DRX. At 1100 °C, the refined DRX grains grow, forming the equiaxed DRX grains. Moreover, the grain orientations are random. DRX grain growth is related to grain boundary migration[17]. With increasing the deformation temperature, the intensity of interface migration and deposition evolution is increased due to the high driving force (Fig. 5b). When the deformation temperature is further increased, the transformation from

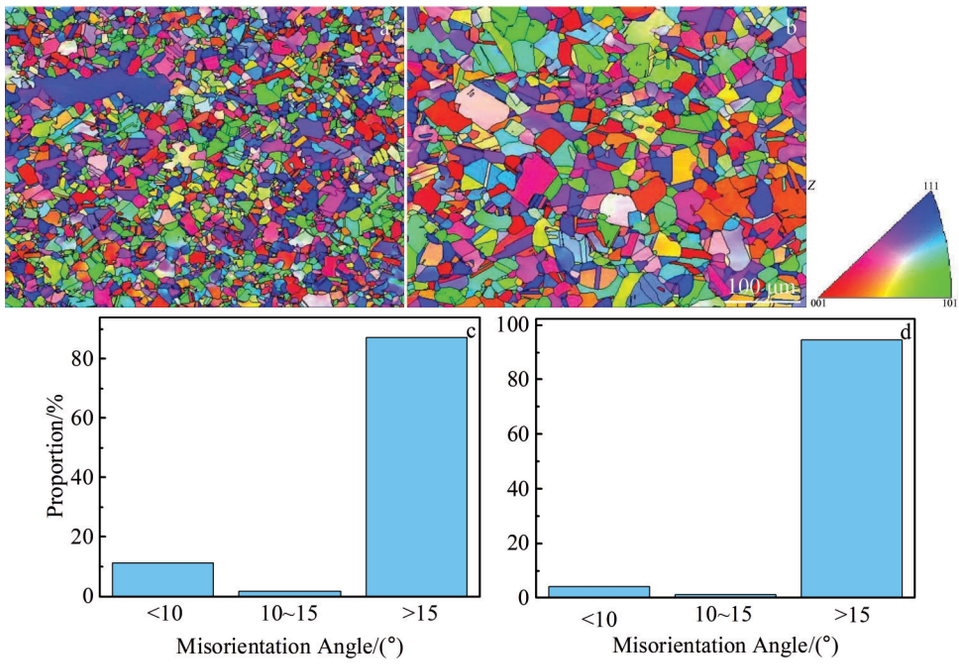

Fig.5 Grain OIMs (a, b) and misorientation analysis results (c, d) at true strain of 0.8 and strain rate of 0.1 s^{-1} with different deformation temperatures: (a, c) 1050 °C and (b, d) 1100 °C

LAGBs to HABGs substantially influences the proportion of LAGBs, which decreases to 4.2% (Fig. 5d). Therefore, DRX can be accelerated at a high deformation temperature[18] .

2.2.3 Deformation degree

The grain boundary misorientation was analyzed under the conditions of deformation temperature of 1000 °C, strain rate of 0.01 s^{-1}, and true strains of 0.2, 0.4, and 0.6. When the true strain is 0.2, the refined DRX grains gather near the bowed grain boundaries and most grain boundaries are LAGBs (Fig. 6a). DRV is the primary softening mechanism of the IN690 alloy[19]. When the thermal compression proceeds, DRX grains replace the original grains, and DRX becomes the primary softening mechanism. All grain boundaries in the microstructure eventually become HAGBs, implying that the essence of continuous DRX (CDRX) is the transformation from LAGBs into HAGBs.

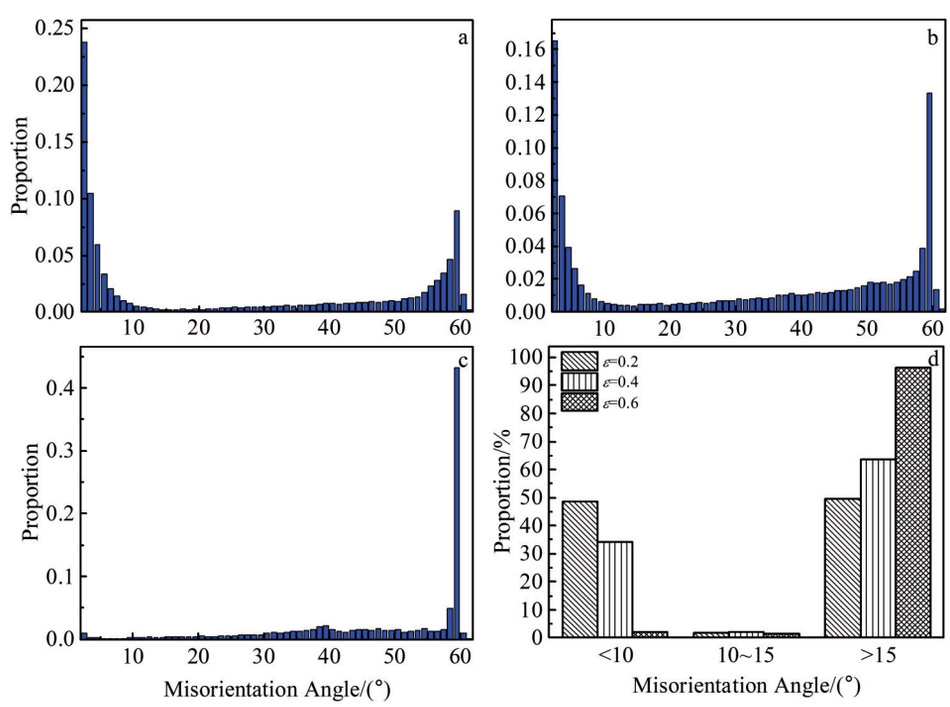

Fig.6 Average misorientation angles under the conditions of 1000 °C/0.01 s^{-1} and different true strains: (a) ε=0.2, (b) ε=0.4, and (c) ε=0.6; comparison of average misorientation angles at different strains (d)

At the true strains of 0.2, 0.4, and 0.6, the average misorientation angles are 26.35°, 31.71°, and 48.76°, and the proportions of LAGBs are 48.7%, 34.3% and 2.26%, respectively. According to Fig. 6d, LAGBs are closely related to the substructures. With the occurrence of DRX, LAGBs are transformed into HAGBs. At a low true strain, the proportion of LAGBs is high and the dislocation accumulation is insufficient to provide enough energy for DRX. After DRX, the substructure absorbs the dislocations in the crystal grains, LAGBs are transformed into HAGBs, the average misorientation angle is increased, and the proportion of LAGBs is decreased.

2.2.4 Microstructure evolution during DRX

Fig. 7 shows the microstructures of IN690 alloy under the deformation conditions of 1000 °C/0.01 s^{-1} and different true strains. LAGBs and HAGBs are represented by the green thin lines and black thick lines, respectively. As shown in Fig. 7a, when the true strain is 0.2, DRX can be observed and most original grains are deformed. Moreover, some newly formed DRX grains appear at the original grain boundaries. Furthermore, the bowed HABGs and fine jagged grain boundaries can be observed. The jagged grain boundaries usually exhibit high local orientations or strain gradients, and they can be arched through the grain boundaries to become potential sites for subsequent nucleation. This is attributed to the grain boundary migration owing to the strain[20]. With the deformation at strain of 0.4, as shown in Fig. 7b, the deformed grains are surrounded by fine DRX grains, forming a necklace structure. Numerous HAGBs can be observed near the bowed grain boundaries, which is the characteristic of discontinuous DRX occurrence during the thermal deformation. Generally, the bowing of the grain boundaries occurs because of energy differences between the adjacent grains. When the strain is 0.6 (Fig. 7c), the bowing of the grain boundary becomes more obvious. Therefore, with increasing the true strain, the stored deformation energy is increased, which increases the driving force for grain boundary migration, and the equiaxed crystals replace the fine recrystallized grains. With the disappearance of the original crystal grains, the uniform and equiaxed crystals are in the dominant position, indicating that complete DRX occurs in the deformed structure.

2.2.5 Grain boundary misorientation during DRX

Typically, CDRX is related to subgrains and dislocations. CDRX behavior of the IN690 alloy is subgrain rotations accompanied by the transformation from LAGBs into HAGBs[21]. Generally, CDRX occurs in deformed grains, and the appearance of MAGBs indicates that CDRX occurs in subgrain. MAGBs are necessary for the occurrence of CDRX. Usually, the subgrain spin nucleation occurs in the grain or at the grain boundary. Therefore, the influence of the true strain on the local and cumulative misorientations parallel and perpendicular to the grain boundary directions was investigated. As shown in Fig. 7a, A1, B1, and C1 lines refer to the misorientation distribution along the grain boundaries, and Al line has the local misorientation of less than 5°. According to Fig. 8a, the cumulative misorientation is nearly 20° . Moreover, the A1 line does not pass through the grain boundary, indicating the DRX mechanism of a progressive subcrystalline rotation and the occurrence of CDRX. A2, B2, and C2 lines refer to the misorientation distribution inside the crystal grains. It can be seen that the local misorientation of A2 is less than 3° , whereas its cumulative misorientation

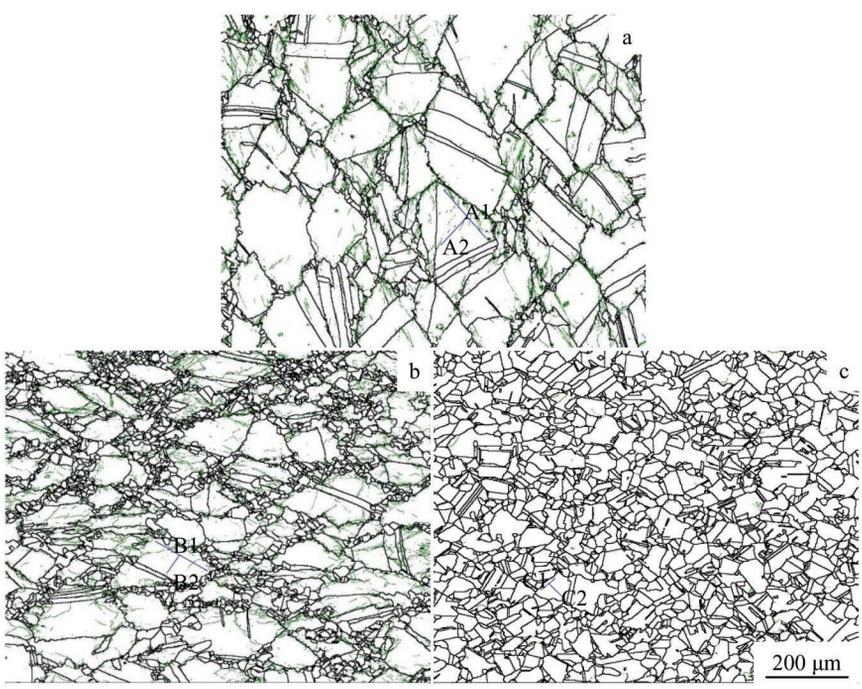

Fig.7 Microstructures of IN690 alloys under the deformation conditions of 1000 °C/0.01 s^{-1} and different true strains: (a) ε=0.2, (b) ε=0.4, and (c) ε=0.6

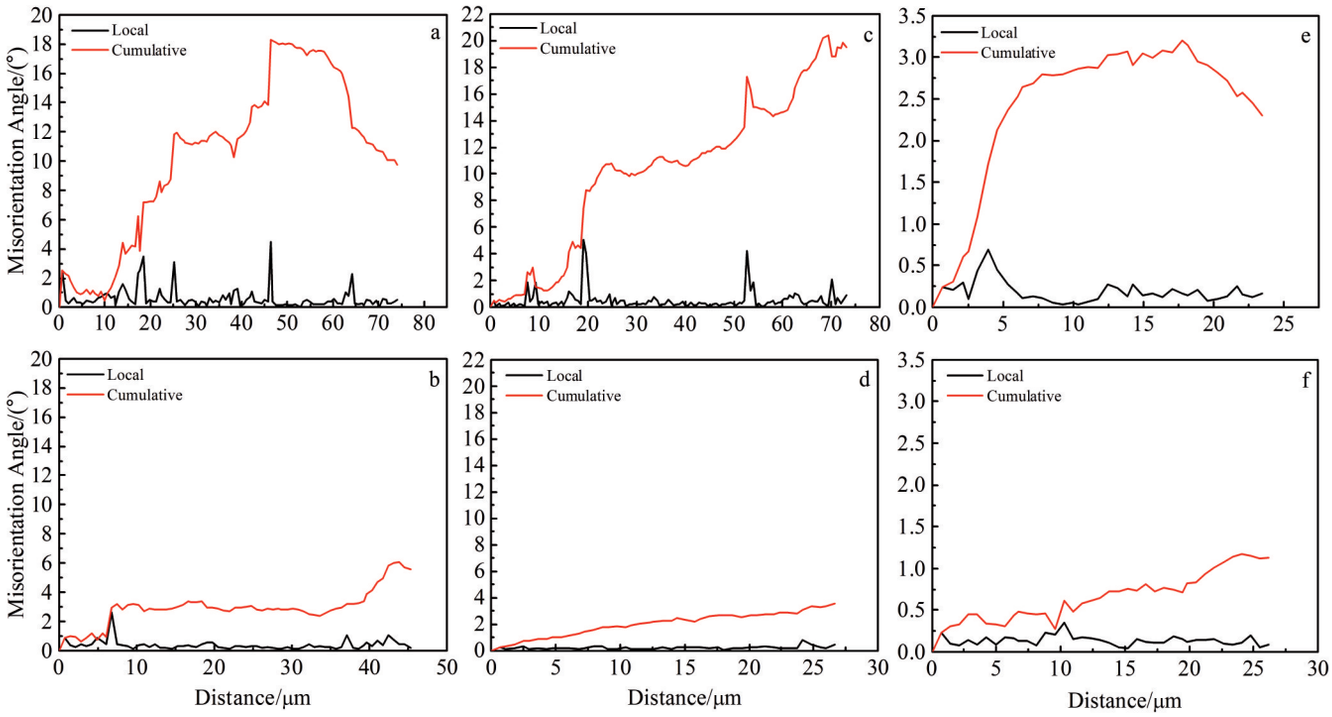

Fig.8 Misorientation angles along different lines in Fig.7: (a) A1, (b) A2, (c) B1, (d) B2, (e) C1, and (f) C2

angle is nearly 7°. The misorientation angles of <15° indicate the occurrence of a small grain rotation inside the crystal grains[22]. When the true strain is 0.4 and 0.6, the cumulative misorientation angle is reduced considerably, indicating that the internal substructure of the grain is consumed, and DRX grains gradually replace the deformed grains.

3 Conclusions

1) The deformation structure of IN690 alloy depends on the deformation parameters. With increasing the true strain and temperature, or with deceasing the strain rate, the deformation storage energy is increased, which provides a strong driving force for the movement of dislocations and boundaries, therefore accelerating the dynamic recrystallization (DRX).

2) Owing to the accumulation of dislocations, the subgrain boundaries constantly absorb the low-angle grain boundaries. Then the local grain misorientation is increased, forming the medium-angle grain boundaries, which gradually become the high-angle grain boundaries. All these transformations lead to the formation of DRX grains.

3) The rearrangement and annihilation of mobile dislocations are accompanied by DRX process and the reduction in low-angle grain boundaries.

References

1 Ahmed M Z, Chadha K, Reddy S R *et al*. *Metallurgical and Materials Transactions A*[J], 2020, 51(12): 6406

2 Liu X D, Fan J K, Li K D *et al*. *Journal of Alloys and Compounds*[J], 2021, 881: 160 648

3 Wang Zhongtang, Zhang Xiaoyu, Deng Yonggang *et al*. *Rare Metal Materials and Engineering*[J], 2014, 43(9): 2252 (in Chinese)

4 Gao P, Chen L L, Luo R *et al*. *Transactions of the Indian Institute of Metals*[J], 2021, 74(11): 2729

5 Zhang Chenghang, Huang Guanjie, Cao Yu *et al*. *Rare Metal Materials and Engineering*[J], 2019, 48(10): 3161

6 Xiao Z B, Huang Y C, Liu Y. *Journal of Materials Engineering and Performance*[J], 2016, 25(3): 1219

7 Eivani A R, Ahmed H, Zhou J *et al*. *Metallurgical and Materials Transactions A*[J], 2009, 40(10): 2435

8 Lin Y C, Nong F Q, Chen X M *et al*. *Vacuum*[J], 2017, 137: 104

9 Xu Meng, Jia Weiju, Zhang Zhihao *et al*. *Rare Metal Materials and Engineering*[J], 2017, 46(9): 2708 (in Chinese)

10 Zhu H J, Chen F, Zhang H M *et al*. *Science China Technological Sciences*[J], 2020, 63(3): 357

11 Zhang F X, Liu D, Yang Y H *et al*. *Modelling and Simulation in Materials Science and Engineering*[J], 2019, 27(3): 35 002

12 Yang Q Y, Ma M, Tan Y B *et al*. *Rare Metals*[J], 2021, 40(10): 2917

13 Wu X, Jiang F C, Wang Z Q *et al*. *Materials Science and Engineering A*[J], 2021, 818: 141 414

14 Zhong L W, Gao W L, Feng Z H *et al*. *Journal of Materials Research*[J], 2018, 33(8): 912

15 Lin Y C, Wu X Y, Chen X M *et al*. *Journal of Alloys and Compounds*[J], 2015, 640: 101

16 Wan Z P, Hu L X, Sun Y *et al*. *Vacuum*[J], 2018, 155: 585

17 Qin F, Feng W, Wu S T. *Ironmaking & Steelmaking*[J], 2018, 45(6): 537

18 Lin Y C, He D G, Chen M S *et al*. *Materials & Design*[J], 2016, 97: 13

19 Chamanfa A, Alamoudi M T, Nanninga N E *et al*. *Materials Science and Engineering A*[J], 2019, 743: 684

20 Jia J B, Yang Y, Xu Y *et al*. *Materials Characterization*[J], 2017, 123: 198

21 Liu P T, Wang R, Liu X D *et al*. *Journal of Materials Engineering and Performance*[J], 2021, 30(2): 1270

22 Jiang J F, Xiao G F, Wang Y *et al*. *Transactions of Nonferrous Metals Society of China*[J], 2020, 30(3): 710

IN690合金在热压缩过程中的再结晶行为

李冬升，赵恩旭，王　威，高　佩，刘　凡

(江苏大学 材料科学与工程学院，江苏 镇江 212013)

摘　要：采用热挤压工艺制备了一种新型高温IN690合金，研究了不同温度、应变速率和变形量对IN690合金动态再结晶（DRX）的影响，利用Gleeble-3500热模拟试验机进行了等轴压缩试验。采用金相显微镜和电子背散射衍射技术，分析了IN690合金热变形前后的金相组织、晶粒取向、晶界分布以及晶粒取向差角。结果表明，随着温度的降低或应变速率的增加，IN690合金的流动应力增加。IN690合金变形过程中的主要软化机制是动态回复和DRX。大角度晶界的比例随着真实应变的增加或应变速率的降低而增加，这是由于在较大的真实应变或相对较低的应变速率下发生了明显的DRX形核。

关键词：IN690；热压缩；微观结构；流动应力；再结晶

作者简介：李冬升，男，1975年生，博士，副研究员，江苏大学材料科学与工程学院，江苏 镇江 212013，E-mail：dsli@ujs.edu.cn